Jiří Jelínek; Karel Segeth; T. R. Overton
Three-dimensional reconstruction from projections

THREE-DIMENSIONAL RECONSTRUCTION FROM PROJECTIONS

Jiří Jelínek, Karel Segeth, T. R. Overton

(Received March 16, 1984)

INTRODUCTION

In many diverse scientific fields, interest has recently been developing in the reconstruction of transaxial images from sets of line integrals. Perhaps the first practical application of the theory [19] was in radio astronomy where brightness temperature maps were reconstructed from interferograms [1]. Later on, in electron microscopy a similar approach made it possible to display molecular biological structures [3]. A most dramatic advance of this method, however, is associated with clinical radiology [9] and nuclear medicine [2].

Known as computerized tomography (CT) or transaxial tomography the technique permits computation and visualization of density (X- or γ-ray absorption coefficients) distribution over a cross-sectional anatomic plane from a set of projections. Three-dimensional reconstruction may then be obtained as a stack of parallel planes. Similarly, emission computerized tomography (ECT) in nuclear medicine provides reconstruction of the three-dimensional distribution of an isotope which has been introduced into the body.

The distribution of some substances (nuclei of hydrogen, phosphorus or sodium) in living organisms can now be displayed using nuclear magnetic resonance [11]. The equivalent of a projection is obtained by the excitation of nuclei in a given anatomic plane and by the Fourier analysis of the resulting NMR signal (nuclear magnetization and relaxation times as given by the Bloch equation) in the presence of magnetic field with linear gradient. By changing the direction of the magnetic gradient, the set of projections is obtained. Since the whole anatomic structure is exposed to the excitation and gradient magnetic fields, the method is intrinsically three-dimensional.

For a physical background of the following theory we shall be referring to standard transmission computed tomography. Minor variations related to other application fields, particularly to NMR tomography, may be found in literature.

Having sets of projection data provided by a particular scanner, the reconstruction of the transverse section requires the selection of an appropriate reconstruction

method according to the geometry of the data collection, the noise in projection data, the amount of data, the computer power available, the accuracy of the reconstruction required by the particular application etc.

Reconstruction methods currently developed may be divided into three groups:

1. arithmetic iterative solutions in the spatial domain [10],
2. reconstructions in the frequency domain [7], [8], and
3. convolution-backprojection in the spatial domain [7], [20], [24]. For ray-sampling schemes of some of the latest tomographic scanners a general linear operator has to be used instead of the convolution [8].

Arithmetic iterative methods behave well with noisy projection data but are only used in special applications owing to the computer time requirements (factor 5 to 10) [13]. For long projection arrays, reconstruction in the frequency domain using the fast Fourier transform may result in a considerable time saving in the convolution step. The use of a transform over the Galois field of integers instead of the usual field of complex numbers in order to reduce round-off errors has been reported [21].

Most of the contemporary tomographs, however, use some kind of the convolution-backprojection algorithm for the following reasons: It is fast and suitable for both parallel and fan-beam data collection geometries (Figures 1 and 2), making possible the reconstruction over a limited region, and, finally, facilitating a mathematical analysis of the noise amplification in the numerical process of reconstruction.

In this paper the theory related to the convolution reconstruction methods is reviewed. A principal contribution consists in the exact mathematical treatment of Radon's inverse transform based on the concepts of the regularization of function and the generalized function developed in [4]. This approach naturally leads to the employment of the generalized Fourier transform in a way similar to [25].

Reconstructions using simulated projection data are presented for both the parallel and the divergent-ray collection geometries.

PROBLEM AND DEFINITIONS

Let us denote the unknown distribution of the X- or γ-ray attenuation density in the transaxial plane (polar coordinates (r, φ)) of the human body by $f(r, \varphi)$. From the source of radiation of the given energy the transmitting ray of η_0 photons per unit length is collimated. Since according to the Lambert-Beer law the decrease of the photon flow along the ray is

$$\mathrm{d}\eta/\mathrm{d}s = -f\eta$$

the detector at the position (l, θ) on the other side of the body detects the mean flux

$$\eta(l, \theta) = \eta_0 \exp\left(-\int_{-\infty}^{\infty} f(\sqrt{(l^2 + s^2)}, \theta + \arctan(s/l))\right) \mathrm{d}s$$

of photons per unit length (Fig. 1).

Considering first the parallel-ray geometry of Fig. 1, the input data is then formed by the set of projections

(1)
$$p(l, \theta) = -\ln \left[\eta(l, \theta)/\eta_0 \right],$$
$$-\infty < l < \infty, \quad 0 \leqq \theta < 2\pi.$$

Each projection defined by a particular value of angle θ corresponds to a subset of parallel evenly spaced projection rays. Clearly,

(2)
$$p(l, \theta) = p(-l, \theta - \pi), \quad \pi \leqq \theta < 2\pi,$$

and thus θ from an interval of length π is to be considered, e.g. $0 \leqq \theta < \pi$. Further, (1) implies

(3)
$$p(l, \theta) = 0, \quad |l| > \varrho,$$

where ϱ is the radius of the disk inside of which the body is placed.

Assuming the function $f(r, \varphi)$ to be continuous, bounded, and zero for $r > \varrho$ with projections $p(l, \theta)$ having the first derivative with respect to l continuous, the problem is to reconstruct the approximation of the attenuation density distribution $f(r, \varphi)$.
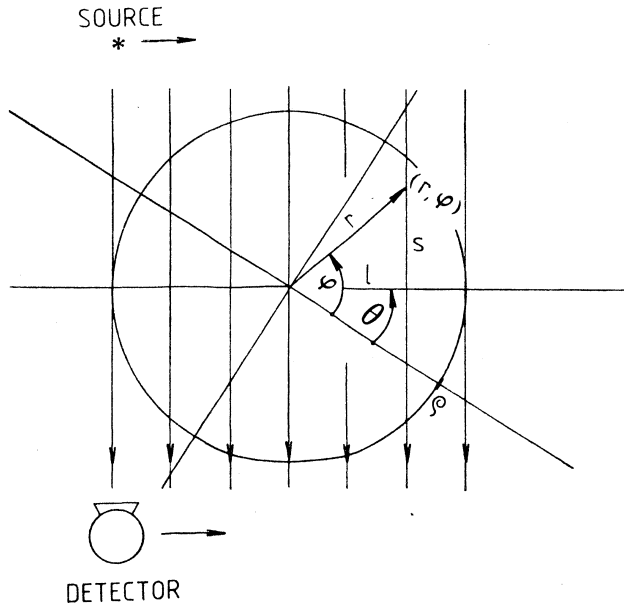

Fig. 1. Parallel-ray projection geometry.

94

All convolution and frequency domain algorithms are various approximate solutions of Radon's inversion formula [19] ([19] is reprinted in full extent e.g. in Helgason [6])

$$(4) \qquad f(r, \varphi) = \frac{1}{2\pi^2} \int_0^\pi \int_{-\infty}^\infty -\frac{1}{l - l'} \frac{\partial}{\partial l} p(l, \theta) \, dl \, d\theta \, ,$$

where $l' = r \cos (\varphi - \theta)$ corresponds to the ray passing through point (r, φ) being reconstructed (Fig. 1). Radon obtained (4) in the form of a Stieltjes integral under more general assumptions. He supposed that $f(r, \varphi)$ is continuous,

$$\int_0^\pi \int_{-\infty}^\infty \frac{1}{r} f(r, \varphi) \, d\varphi \, dr < \infty \, ,$$

and that, for any point (r_0, φ_0) of the plane, the integral of $f(r, \varphi)$ along a circle with center (r_0, φ_0) and radius R converges to zero as $R \to \infty$. The form (4) can be obtained from the original Radon's results if $\partial p(l, \theta)/\partial l$ is continuous.

Note that the assumptions of the previous section guarantee that all these conditions are satisfied. The theory of regularization of functions based on the concept of generalized functions (established e.g. in [4], [23]) enables us to give the formula (4), where the integrand possesses a singularity at $l = l'$, a clear meaning.

In [4] the theory of the regularization of functions is developed with the test function space D of infinitely smooth functions ψ having a compact support. The principal idea is the following. A function u to be regularized is treated as a functional and formally represented by the integral

$$I_u(\psi) = \int_{-\infty}^\infty u(x) \psi(x) \, dx \, ,$$

where $\psi \in D$, which may not exist for some ψ. The integral $I_u(\psi)$ is extended to all $\psi \in D$ with the help of a suitably chosen integral $\hat{I}(_u\psi)$, the regularization of $I_u(\psi)$, which exists in the usual sense for all $\psi \in D$ and

$$(5) \qquad \hat{I}_u(\psi) = I_u(\psi)$$

if $I_u(\psi)$ exists. If $I_u(\psi)$ does not exist for some $\psi \in D$ then (5) is taken for the definition of $I_u(\psi)$. In this way, I_u as well as u (in the sense of a functional) are regularized. In our case the results can be extended to all continuous functions ψ, too. Employing this approach, we replace the inner integral in (4) by its regularization ([4], Ch. I, § 3)

$$(6) \qquad \int_0^\infty -\frac{1}{l} \left(\frac{\partial}{\partial l} p(l + l', \theta) - \frac{\partial}{\partial l} p(-l + l', \theta) \right) dl \, .$$

Rewrite (6) as

$$\lim_{\varepsilon \to 0+} \int_{\varepsilon}^{\infty} - \frac{1}{l}\left(\frac{\partial}{\partial l}\, p(l + l', \theta) - \frac{\partial}{\partial l}\, p(-l + l', \theta)\right) \mathrm{d}l = \lim_{\varepsilon \to 0+} J(\varepsilon, l', \theta)\,.$$

Integrating by parts for fixed l' and θ, we obtain

$$J(\varepsilon, l', \theta) = \frac{1}{\varepsilon}\left(p(\varepsilon + l', \theta) + p(-\varepsilon + l', \theta)\right) - \int_{\varepsilon}^{\infty} \frac{1}{l^2}\left(p(l + l', \theta) + p(-l + l', \theta)\right) \mathrm{d}l$$

since $1/l^2$ as well as $\partial p(l + l', \theta)/\partial l - \partial p(-l + l', \theta)/\partial l$ are continuous in $\langle \varepsilon, \infty)$ and both the left-hand side and $\left(p(\varepsilon + l', \theta) + p(-\varepsilon + l', \theta)\right)/\varepsilon$ exist for any fixed $\varepsilon > 0$.

As

$$\int_{\varepsilon}^{\infty} \frac{1}{l^2}\, \mathrm{d}l = \frac{1}{\varepsilon}$$

we may write

$$J(\varepsilon, l', \theta) = \int_{\varepsilon}^{\infty} - \frac{1}{l^2}\left(p(l + l', \theta) + p(-l + l', \theta) - \right.$$
$$\left. - p(\varepsilon + l', \theta) - p(-\varepsilon + l', \theta)\right) \mathrm{d}l\,.$$

The conditions necessary for passing to the limit in $J(\varepsilon, l', \theta)$ (cf. e.g. Jarník [12], Ch. VIII, § 4) are satisfied and we finally obtain that (6) can be expressed as

(7) $$\int_{0}^{\infty} - \frac{1}{l^2}\left(p(l + l', \theta) + p(-l + l', \theta) - 2p(l', \theta)\right) \mathrm{d}l\,,$$

which is the regularization of the integral (cf. [4])

(8) $$\int_{-\infty}^{\infty} - \frac{1}{(l - l')^2}\, p(l, \theta)\, \mathrm{d}l = \int_{-\infty}^{\infty} q(l - l')\, p(l, \theta)\, \mathrm{d}l\,,$$

where

(9) $$q(l) = - \frac{1}{l^2}\,.$$

Using the notation (8), we always mean the regularization (7) of this integral.

Note that according to [4], Ch. I, § 3 we obtain

(10) $$\int_{-\infty}^{\infty} q(l)\, \mathrm{d}l = 0$$

if the integral on the left-hand side is replaced by its regularization. Since (10) is the integral mean of (the regularization of) the function $q(l) = -1/l^2$ we conclude that this mean is zero.

Turning back to the formula (4), we can rewrite it in accord with (6), (7), and (8) as

$$(11) \qquad f(r, \varphi) = \frac{1}{2\pi^2} \int_0^\pi \int_{-\infty}^\infty q(l' - l) \, p(l, \theta) \, \mathrm{d}l \, \mathrm{d}\theta \, .$$

Now, (11) is the continuous reconstruction formula in spatial domain. It implies that the contribution of each projection $p(l, \theta)$ to the value of the reconstruction at the point (r, φ) is weighted by the negative squared inverse of its distance from that point.

In practical reconstructions, various regularizations of (8) are used [20]. The well known discrete spatial convolver of Shepp and Logan [24] has been obtained from (8) by approximating the convolution integral by the sum of integrals over the beam width assuming constant values of the projection integrals in these subintervals. Obviously other approximations using more realistic beam profiles can be derived. Generally, however, the function q is replaced by a continuous function q_ε having no singularity, depending on the parameter ε and satisfying the condition (10).

It can be readily seen that the inner integral in (11) is a convolution of the functions q and p. This is the fact which is often used to evaluate (11) efficiently with the help of the Fourier transform.

We introduce the one-dimensional Fourier transform $\mathscr{F}(u) = v$ of a function u from S, the space of infinitely smooth functions rapidly decreasing in infinity together with all their derivatives, and its inverse $\mathscr{F}^{-1}(v) = u$ as

$$v(t) = \int_{-\infty}^\infty u(x) \exp(2\pi i x t) \, \mathrm{d}x \, ,$$

$$u(x) = \int_{-\infty}^\infty v(t) \exp(-2\pi i x t) \, \mathrm{d}t$$

and generalize it to distributions [26]. Then we find out that under our assumptions the Fourier transform P of p (θ is considered a parameter) exists,

$$(12) \qquad P(R, \theta) = \int_{-\infty}^\infty p(l, \theta) \exp(2\pi i l R) \, \mathrm{d}l$$

and that the generalized Fourier transform Q of the function q ([4], Ch. II, § 2; [25]) exists as well,

$$Q(R) = 2\pi^2 |R| \, .$$

Employing the well-known formula for the Fourier transform of a convolution

$$\mathscr{F}(u_1 * u_2) = \mathscr{F}(u_1) \, \mathscr{F}(u_2) \, ,$$

we obtain the frequency domain version of (11) in the form

$$(13) \qquad f(r, \varphi) = \int_0^\pi \int_{-\infty}^\infty P(R, \theta) \, |R| \exp\left(-2\pi i r R \cos(\theta - \varphi)\right) \, \mathrm{d}R \, \mathrm{d}\theta \, .$$

In practical discrete implementations of numerical reconstruction, a regularization of (8) (or (11)) may be obtained if q is replaced by q_W, the inverse Fourier transform of Q_W, which is a properly modified function Q. We put

$$(14) \qquad Q_W(R) = 2\pi^2 |R| \, W(R/C) \,,$$

$$(15) \qquad q_W(l) = \int_{-\infty}^{\infty} Q_W(R) \exp\left(-2\pi i l R\right) \mathrm{d}R \,,$$

where $W(t)$ is the window function, i.e. a smooth function vanishing for $|t| > 1$, which appropriately modifies the behavior of the $|R|$-filter $Q(R)$, and C is the Nyquist frequency in the discrete Fourier transform employed, i.e. the cut-off frequency. The formula (14) implies that (10) holds for q_W as $Q_W(0) = 0$. Finally we get the spatial filter (15) in the form

$$(16) \qquad q_W(l) = 2\pi^2 \int_{-C}^{C} |R| \, W(R/C) \exp\left(-2\pi i l R\right) \mathrm{d}R \,.$$

Examining the formula (11), we see that it is advantageous to carry out the reconstruction in two separate steps:

1. The inner integral (convolution)

$$(17) \qquad g(l', \theta) = \int_{-\infty}^{\infty} q(l' - l) \, p(l, \theta) \, \mathrm{d}l \,,$$

called the corrected projection, is evaluated first. In practical computation, we use e.g. q_W given by (16) instead of q. The approximate corrected projection is then denoted by g_W.

2. The reconstructed approximation of the density $f(r, \varphi)$ is obtained by the back-projection (superposition) of these corrected projections for all values of θ, i.e.,

$$(18) \qquad f(r, \varphi) = \frac{1}{2\pi^2} \int_0^{\pi} g(l', \theta) \, \mathrm{d}\theta \,,$$

and, replacing here g by g_W, we come to the approximation f_W.

The above conclusions concerned with the computation of f_W with the help of (11) or (13) can be summarized if we introduce the backprojection operator $\mathscr{B}$ as

$$\mathscr{B}(u) = \frac{1}{2\pi^2} \int_0^{\pi} u(\theta) \, \mathrm{d}\theta \,.$$

Then (11) may be rewritten as the so-called convolution-backprojection

$$f_W = \mathscr{B}(q_W * p) \,.$$

and (13) becomes the so-called backprojection of filtered projections

$$(19) \qquad f_W = \mathscr{B}\left(\mathscr{F}^{-1}\left(Q_W \, \mathscr{F}(p)\right)\right) \,,$$

where we use the notation (14) and (15).

An alternative algorithm applying the backprojection operator directly to the set of measured projections was also studied [5]. In contrast to (19), the Fourier transform employed is now two-dimensional and Q_W is replaced by a suitable function depending only on the distance from the origin in the image plane (i.e. a two-dimensional circularly symmetric filter).

DIVERGENT RAY GEOMETRY

The use of first generation scanners with parallel-ray geometry is limited to measuring stationary anatomic structures only since the data collection time is of the order of minutes. Research concerning the three-dimensional display of moving organs (such as lungs and heart) together with the need for the evaluation of other dynamical processes necessitated the construction of fast scanners using divergent ray geometry (Fig. 2).
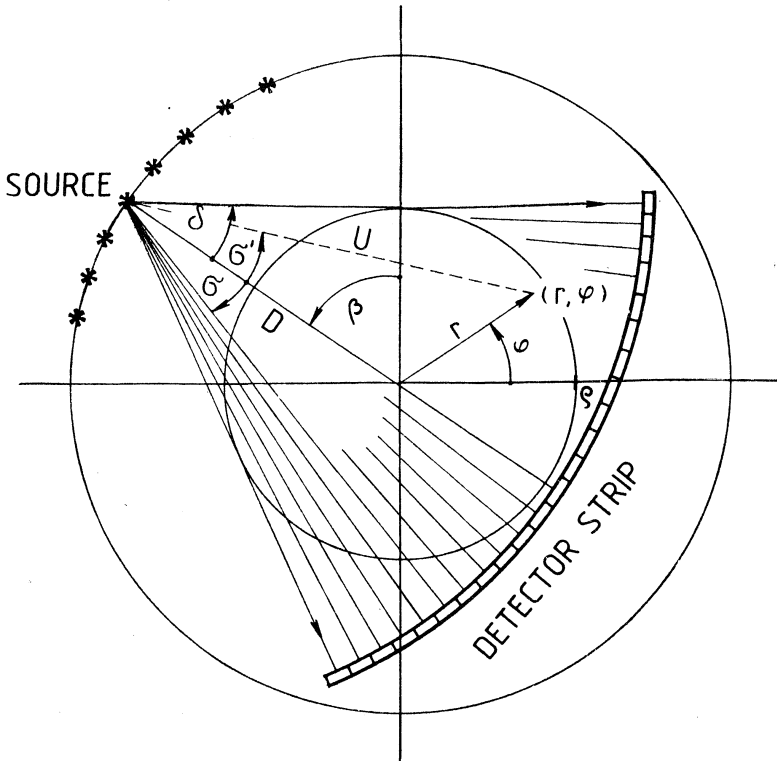
Fig. 2. Divergent-ray projection geometry.

A reconstruction algorithm for scanners where projections were obtained from a single source and evenly spaced detectors was for the first time suggested by Lakshminarayanan in 1975 (Technical Report 92, Department of Computer Science, State University of New York at Buffalo). The reader is referred to the rigorous derivation given e.g. by Herman et al. in [7]. Computer experiments discussed in the last section, however, use the straightforward approach of Lewitt [16] as briefly described below.

Referencing the diverging ray by the angle β defining the source position and by the angle of divergence σ, the line integral of a divergent projection can be denoted by $p^*(\sigma, \beta)$, $p^*(\sigma, \beta) = 0$ for $\sigma > \delta$. From Fig. 2 (l and θ have the same meaning as in Fig. 1, $l = D \sin \sigma$, $\theta = \beta + \sigma$)

$$r \cos (\theta - \varphi) - l = U \sin (\sigma' - \sigma)$$

where the distance between the source and the point (r, φ) is

$$U = ([r \cos (\beta - \varphi)]^2 + [D + r \sin (\beta - \varphi)]^2)^{1/2}$$

and the angle of divergence σ' for the ray passing through (r, φ) is

$$\sigma' = \arctan [r \cos (\beta - \varphi)/(D + r \sin (\beta - \varphi))] .$$

The transformation of coordinates (l, θ) into (σ, β) in (12) and (13) yields, with regard to (3), the reconstruction formula

$$f_W(r, \varphi) =$$

$$= \frac{D}{2} \int_{-\infty}^{\infty} \int_{-\delta}^{\delta} \int_{0}^{2\pi} p^*(\sigma, \beta) \cos \sigma \exp [-2\pi i R U \sin (\sigma' - \sigma)] W(R/C) |R| \, d\beta \, d\sigma \, dR ,$$

where $p^*(\sigma, \beta) = p(D \sin \sigma, \beta + \sigma)$. The relation (2) cannot be used for p^*.

Changing the order of integration, the reconstruction can again be carried out in two steps:

1. The convolution step has the form

(20) $$g_W(\sigma', \beta) = \int_{-\delta}^{\delta} p^*(\sigma, \beta) \cos \sigma \, q_W(U \sin (\sigma' - \sigma)) \, d\sigma .$$

2. The reconstructed value of density at the point (r, φ) is obtained by back-projection

$$f_W(r, \varphi) = \frac{D}{4\pi^2} \int_{0}^{2\pi} g_W(\sigma', \beta) \, d\beta .$$

The efficient implementation of the above algorithm requires, however, the separation of the U-dependent component of the filter, i.e. the filter of the form

(21) $$q_W(U \sin \sigma) = q^B(C, U) \, q^F(\sigma)$$

where the component $q^B(C, U)$ can be applied as a multiplicative weight in the back-projection step and C is given in (14), (15).

Separation of the U-dependent component of the spatial filter in (20) as advocated by Lewitt [16], however, sacrifices the uniform resolution of the final reconstruction. When the substitution $R' = RU \sin \sigma/(D\sigma)$ is performed in (16), then

$$q_W(U \sin \sigma) = 2 \left[\frac{D}{U} \frac{\sigma\pi}{\sin \sigma} \right]^2 \int_{-\chi}^{\chi} |R'| \, W(R'/C) \exp\left(-2\pi i D\sigma R' \right) \mathrm{d}R',$$

which obviously satisfies (21). The new cut-off frequency

$$\chi(C, U, D, \sigma) = CU \frac{\sin \sigma}{D\sigma}$$

would for $C = \text{const}$ vary with U. Making $\chi = \text{const}$ means to accept uneven resolution over the region of reconstruction. This approximate approach, however, facilitates an easy adaptation of any "parallel" filter $|R| \, W(R/C)$ to the divergent-ray geometry. Generally the regularization of the divergent reconstruction formula reduces the inner integral to a convolution only for the special choice of the regularizing kernels [7].

DISCRETE IMPLEMENTATION

In practice tomographic scanners produce only finite number of projections and rays per projection. The integrals in the reconstruction formulae have therefore to be approximated by finite sums. Assuming the parallel-ray geometry with an even spacing a between the parallel rays over the whole scanned region and an even increment $\Delta\theta = \pi/M$ between projections, we denote the discrete values of the projection (1) by

$$p_{kj} = p(ka, \theta_j),$$

$$k = 0, 1, \ldots, N - 1; \quad \theta_j = j \, \Delta\theta, \quad j = 0, 1, \ldots, M - 1.$$

The discrete approximation of the reconstructed attenuation density (11) at a point (r, φ) is then obtained with the help of the trapezoidal formula in the form

$$(22) \qquad f(r, \varphi) \approx \frac{a}{2\pi M} \sum_{j=0}^{M-1} \sum_{k=0}^{N-1} q_{k'-k} p_{kj}$$

where $k' - k$ corresponds to the distance $l' - l$ from the kth ray to the point of reconstruction, $q_m = q(ma)$.

Since $k'a$ and $l'_j = r \cos(\theta_j - \varphi)$ as well as the corresponding values of the corrected projections $g(k'a, \theta_j)$ and $g(l', \theta_j)$ in (17) coincide only when the k'th ray passes through the point (r, φ) of the reconstruction, some kind of interpolation must be introduced in the discrete backprojection step of (22) in order to be able to

compute the density values on the fixed reconstruction matrix. It is obvious that the quality of the reconstructed approximation will be influenced by both the $|R| W(R)$ convolution filter and by the interpolation filter.

The spatial filter $q(ka)$ can be obtained either as the result of an appropriate regularization in the spatial domain or, more generally, by the inverse Fourier transform (16) of the filter $|R| W(R)$ in the frequency domain.

From (9) and (10) it follows that, under the assumption of the continuity of the first partial derivative of $p(l, \theta)$ with respect to l, the accurate reconstruction may be obtained by the $|R|$-filter, provided that the frequency spectrum of the $f(r, \varphi)$ is bounded well below the Nyquist frequency $C_N = 1/(2a)$ given by the sampling interval a, and that the accurate interpolation given by the sampling theorem is applied.

In practice, however, these assumptions are often violated due to the statistical fluctuations in the projection data. The spectrum of the input noise is usually shifted towards higher frequencies and therefore the noise is amplified by the $|R|$-filter. Since the harmonic components of the projections containing useful information are in an interval closer to the zero frequency, it is desirable to modify the $|R|$-filter by an appropriate window $W(R)$. Various forms of Hamming, Hanning, Butherworth
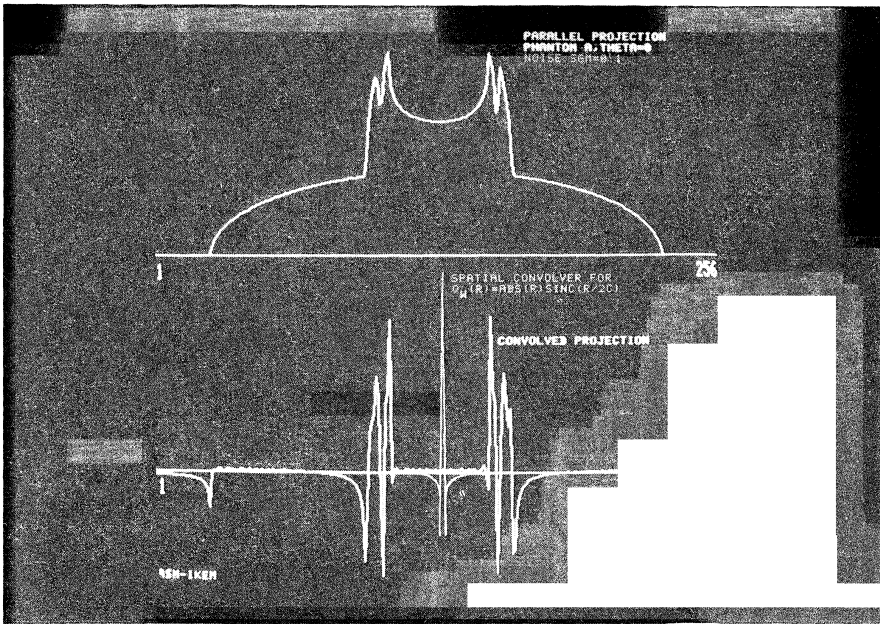

Fig. 3. Top: Projection $p(ka, 0)$ of phantom A of Fig. 7a.
Bottom: Corrected projection $g(ka, 0)$ (bold line) with spatial convolver $q_W(ka)$ for the window (23) (light line).

102

etc. window functions may provide useful approximations of the exact reconstruction. In many practical applications, however, best results were obtained with the window suggested by Shepp and Logan [24]

$$(23) \qquad\qquad W(R/C) = \operatorname{sinc}\left(R/(2C)\right),$$

where $\operatorname{sinc} x = \sin \pi x / (\pi x)$. This window function corresponds to the discrete spatial filter $q_{k'-k}$ obtained from (8) by the approximation of the integral using the sum of integrals over the beam width with constant values p_{kj}. The value of the singular coefficient q_0 has to satisfy (10). Using (23) together with the linear interpolation in the backprojection step, a discrete filtration by the filter

$$(24) \qquad\qquad |R| \operatorname{sinc}\left(R/(2C)\right) \operatorname{sinc}^2\left(R/(2C)\right)$$

is then effectively performed on the input projection data. The last squared term in (24) may be interpreted as a triangular function which is being implicitly convolved with the discrete projection data to obtain a continuous piecewise linear output from the digital filter corresponding to the linearly interpolated discrete projection data. The graphs of a projection, corrected projection and the spatial convolver corresponding to the filter $Q_W(R) = |R| \operatorname{sinc}\left(R/(2C)\right)$ are shown in Fig. 3.
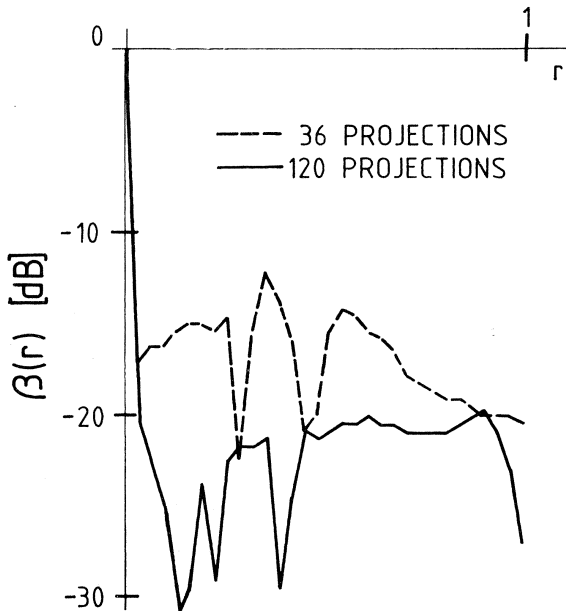

Fig. 4. Logarithm $\beta(r)$ of normalized line spread function for $W(R/C) = \operatorname{sinc}\left(R/(2C)\right)$. Parallel-ray geometry, 36 and 120 projections, 127 rays per projection.

In the parallel and divergent-ray geometries discussed above, uniform sampling in coordinates (l, θ) and (σ, β), respectively, was considered. The corresponding convolution reconstruction algorithms are therefore linear [8]. Since the projection measurement process is assumed to be also linear, the principle of superposition holds in the sense that the final reconstruction is the superposition of the point spread functions $S(r, \varphi)$ (reconstruction of the δ-function at the point (r, φ)) corresponding to all points (r, φ) of the original. The simplest criterion for the evaluation of the reconstruction algorithms is therefore the reconstruction of the δ-function located at the center of the reconstruction matrix, particularly the behavior of $S(r, \varphi)$ for $r > 0$ where, for the ideal case of infinite number of projections, the backprojected corrected projections should cancel out. The discrete one-dimensional representations $S(r, 0)$ or, more specifically, the logarithms of their normalized form

$$\beta(r) = 10 \log |S(r, 0)/S(0, 0)| , \quad r = na , \quad n = 0, 1, ..., 31 ,$$

for 36 and 120 projections are compared in Fig. 4 for $W(R/C) = \text{sinc}(R/(2C))$ and the parallel-ray geometry. The reconstruction of the δ-function from divergent-ray projections using the window function

$$(25) \qquad W(R/C) = 1 - \varepsilon|R/C| , \quad 0 \leqq \varepsilon \leqq 1 ,$$

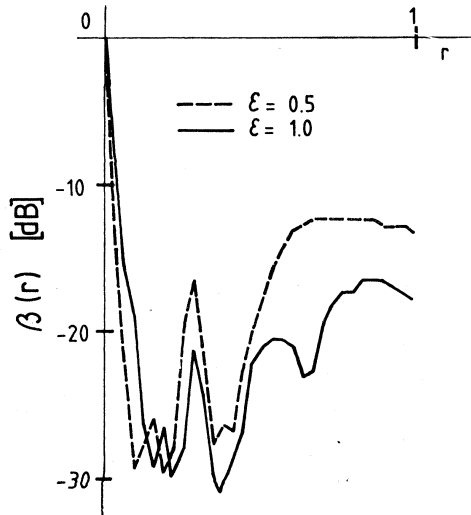is shown in Fig. 5. In both the examples, corrected projections comprising 127 line

Fig. 5. Logarithm $\beta(r)$ of normalized line spread function for $W(R/C) = 1 - \varepsilon|R/C|$. Divergent-ray geometry, 120 projections, 127 rays per projection.

integrals (rays) per projection, where only the integral along the 64th ray was non-zero, were backprojected into a 64 × 64 reconstruction matrix.

An increase in the projection sampling density in noiseless projection data narrows the point spread function and thus improves the overall quality of the reconstructed image. In case of the noisy projection data of a real scanner, however, the spatial averaging provided by the finite width of projection rays effectively functions as a low-pass filter.

An increase in the number of projections lowers the residual oscillations over the reconstruction matrix. In Fig. 4, approximately a 10 dB difference can be observed between the reconstructions from 36 and 120 projections.
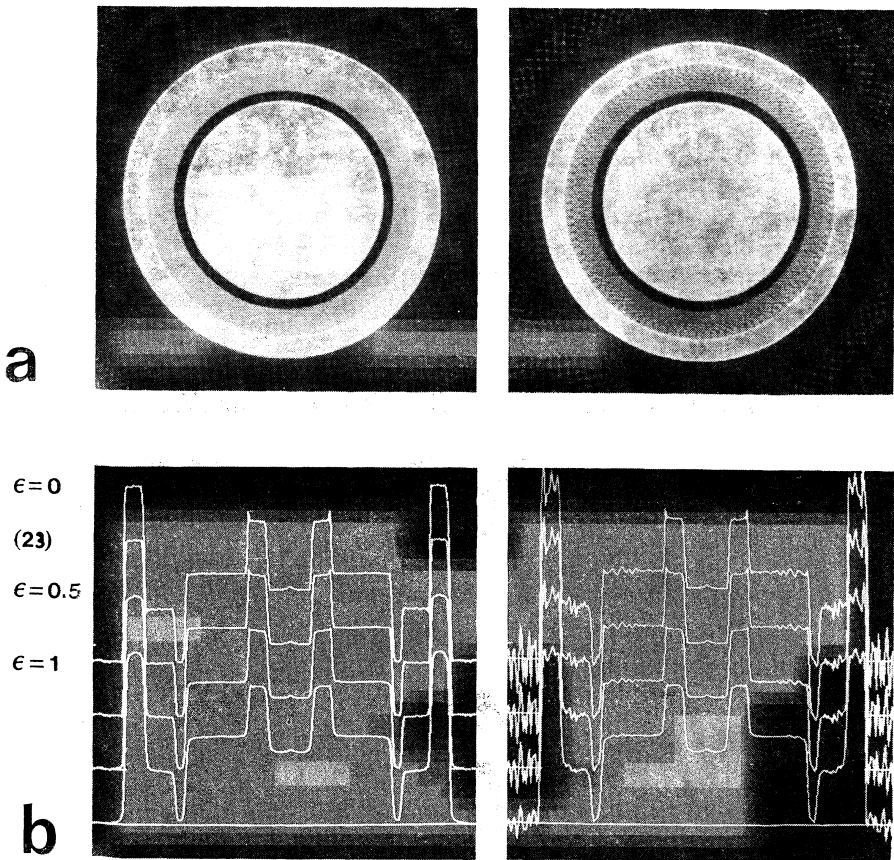

Fig. 6. a) Circularly symmetric phantom reconstructed from 56 (right) and 112 (left) parallel projections. b) Horizontal profiles for window functions $W(R/C) = 1 - \varepsilon |R/C|$, $\varepsilon = 1$, 0·5, 0, and window function (23).

In the following experiment the parallel-ray projections of a circularly symmetric phantom were computed with the projection sampling density 256 rays per projection. Reconstructions according to the relations (17), (18) were carried out for the window functions (23) and (25), where the values of the parameter ε were chosen 0 (RAMP filter), 0.5 and 1. Reconstructed profiles in Fig. 6b demonstrate a decrease of spatial frequency content with increasing ε. This is in agreement with the character of the corresponding window functions. Reconstructed profiles also demonstrate a decrease of the artifacts outside the dense ring and an overall increase of the reconstruction accuracy with an increasing number of projections. These artifacts are due to the fact that whenever a circular or elliptical object is reconstructed by a convolution method [20] the superimposed corrected projections have much
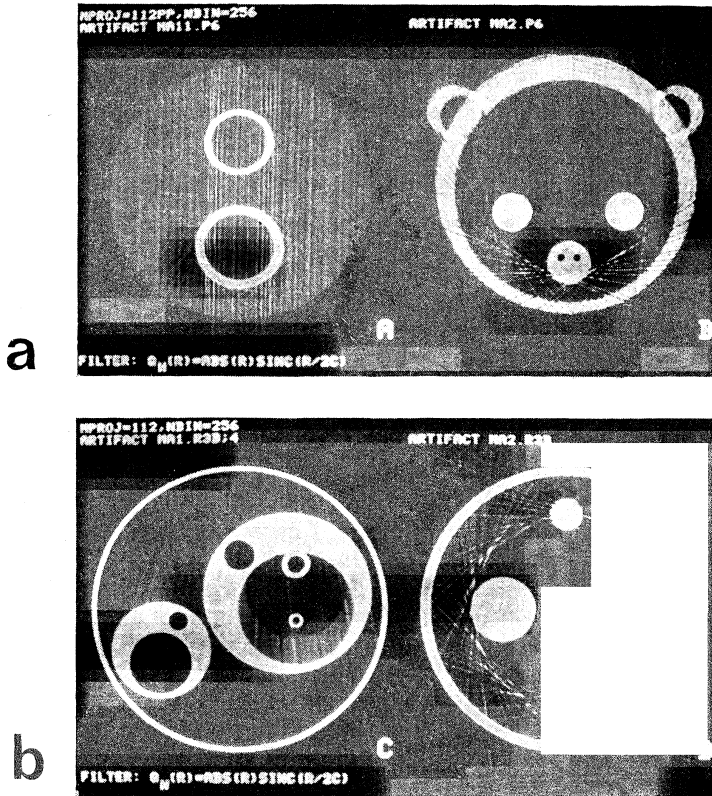

Fig. 7. Reconstruction of mathematical phantoms from a projection set (112 projections, 256 rays per projection) with Gaussian additive noise in the last projection (left) and in ray 64 of all projections (right); filter $Q_W(R) = |R|\sin c\,(R/(2C))$: a) parallel-ray geometry; b) divergent-ray geometry.

greater values outside the object than inside (see the negative peaks of the corrected projection in Fig. 3).

Characteristic artifacts shown in Fig. 7 were obtained by introducing noise into one projection from the projection set, or into "one detector" when each projection from the projection set had one bad projection ray with additive noise.

ERRORS OF RECONSTRUCTION — DISCUSSION

Degradation of the reconstructed image in tomographic systems depends on the measured object itself, on the fundamental parameters of the scanner (ray profile, number of rays and projections, alignment of the scanner, etc.) and on the reconstruction algorithm.

The most often violated assumption of Radon's inversion formula (4) is the continuity of the partial derivative of the projection $p(l, \theta)$ with respect to l. As a result the characteristic artifacts then appear between the dense edges of the reconstructed image.

High concentrations of contrast material in the object produce significant beam hardening artifacts due to polychromaticity of the photon beam. These artifacts appear as dark, relatively unmodulated zones between these contrast structures. They are the more pronounced, the more the energy-dependent attenuation coefficients vary, the greater their absolute values are, and the more extensive these structures are. The relatively clear origin of these artifacts has made it possible to develop several correction methods [22].

In situations where the value of the projection integral varies significantly in the direction perpendicular to the transverse section, partial volume streak artifacts appear between pairs of the structures that only partially fill up the volume of the ray [15]. In contrast to the above mentioned artifacts due to the energy dependence of attenuation, the partial volume effect manifests itself as both light and dark highly modulated streaks. These streaks can be greatly reduced when the projection data from narrow slices is used for reconstruction.

The discrete sampling of projections in the data acquisition process results in a periodic frequency spectrum and in the loss of information about frequencies higher then the Nyquist frequency given by the sampling interval. The resulting aliasing and loss of spatial invariance of the point spread function can be reduced by making the sampling interval sufficiently small. For noisy projection data, however, an appropriate compromise must be chosen [14].

[1] *R. N. Bracewell, A. C. Riddle:* Inversion of fan-beam scans in radio astronomy. Astrophys. J. 150 (1967), 427—434.

[2] *T. F. Budinger, G. T. Gullberg:* Three-dimensional reconstruction in nuclear medicine emission imaging. IEEE Trans. Nucl. Sci. NS-21 (1974), 2—20.

[3] *D. De Rosier, A. Klug:* Reconstruction of three-dimensional structures from electron micrographs. Nature 217 (1968), 130—138.

[4] *I. M. Gel'fand, G. E. Šilov:* Generalized functions and operations on them. (Russian.) Gos. izd. fiz.-mat. lit., Moskva 1959.

[5] *G. T. Gullberg:* The reconstruction of fan-beam data by filtering the back-projection. Comput. Graphics and Image Process. 10 (1979), 30—47.

[6] *S. Helgason:* The Radon transform. Birkhäuser, Boston 1980. (Russian translation: Mir, Moskva 1983.)

[7] *G. T. Herman, A. V. Lakshminarayanan, A. Naparstek:* Convolution reconstruction techniques for divergent beams. Comput. Biol. Med. 6 (1976), 259—271.

[8] *B. K. P. Horn:* Fan-beam reconstruction methods. A. I. Memo No. 448, Massachusetts Institute of Technology, 1977.

[9] *G. N. Hounsfield:* Computerized transverse axial scanning (tomography). Part I: Description of system. British J. Radiol. 46 (1973), 1016—1022.

[10] *R. H. Huesman, G. T. Gullberg, W. L. Greenberg, T. Budinger:* Donner algorithms for reconstruction tomography. Tech. Rpt. Pub. 214, Lawrence Berkeley Laboratory, 1977.

[11] *J. E. Husband, I. K. Fry:* Computed tomography of the body. Mac Millan Publishers 1981.

[12] *V. Jarnik:* Integrální počet II. Nakladatelství ČSAV, Praha 1955.

[13] *J. Jelínek, T. R. Overton:* Comparative study on reconstruction from projections: Correction functions. Proceedings Colloquium on Mathematical Morphology, Stereology and Image Analysis, ČSAV, Prague 1982, 113—116.

[14] *P. M. Joseph, R. D. Spital:* The exponential edge-gradient effect in X-ray computed tomography. Phys. Med. Biol. 3 (1981), 473—487.

[15] *P. M. Joseph, R. D. Spital, C. D. Stockham:* The effects of sampling on CT images. Comput. Tomogr. 4 (1980), 189—206.

[16] *R. M. Lewitt:* Ultra-fast convolution approximations for image reconstruction from parallel and fan beam projection data. Technical Report No. MIPG25, Medical Imaging Processing Group, Dept. of Computer Science, State University of New York at Buffalo, 1979.

[17] *R. M. Lewitt, R. H. T. Bates:* Image reconstruction from projections II: Modified back-projection methods. Optik 50 (1978), 85—109.

[18] *R. M. Mersereau:* Direct Fourier transform techniques in 3-D image reconstruction. Comput. Biol. Med. 6 (1976), 247—258.

[19] *J. Radon:* Über die Bestimmung von Funktionen durch ihre Integralwerte langs gewisser Manningfaltigkeiten. Ber. Verh. Saechs. Akad. Wiss. Leipzig, Math.-Nat. Kl., 69 (1917), 262—277.

[20] *G. N. Ramachandran, A. V. Lakshminarayanan:* Three-dimensional reconstruction from radiographs and electron micrographs: Application of convolutions instead of Fourier transforms. Proc. Nat. Acad. Sci. U.S.A. 68 (1971), 2236—2240.

[21] *I. S. Reed, Y. S. Kwoh, T. K. Truong, E. L. Hall:* X-ray reconstruction by finite field transforms. IEEE Trans. Nucl. Sci. NS-24 (1977), 843—849.

[22] *P. Rüegsegger, T. N. Hangartner, H. U. Keller, et al.:* Standardization of computed tomography images by means of material-selective beam hardening correction. J. Comput. Assist. Tomogr. 2 (1978), 184—188.

[23] *L. Schwartz:* Théorie des distributions 1 & 2. Hermann, Paris 1950, 1951.

[24] *L. A. Shepp, R. F. Logan:* The Fourier reconstruction of a head section. IEEE Trans. Nucl. Sci. NS-21 (1974), 21—43.

[25] *E. Tanaka:* Generalized correction functions for convolutional techniques in three-dimensional image reconstruction. Phys. Med. Biol. 24 (1979), 157—161.

[26] *K. Yosida:* Functional analysis. Springer-Verlag, Berlin 1965.

Souhrn

TROJROZMĚRNÁ REKONSTRUKCE Z PROJEKCÍ

JIŘÍ JELÍNEK, KAREL SEGETH, T. R. OVERTON

Počítačová tomografie je technika pro výpočet a zobrazení rozložení určité vlastnosti objektu (např. koeficientu absorpce u CT nebo protonové hustoty u NMR) v příčném rovinném řezu pomocí projekcí. Trojrozměrné rekonstrukce se dosáhne použitím systému rovnoběžných rovin.

K rekonstrukci příčného řezu je třeba zvolit metodu vhodnou s ohledem na geometrii, v níž byla pořízena data, šum v datech, množství dat, schopnosti počítače, který je k dispozici, požadovanou přesnost rekonstrukce atd.

V článku je přehledně uvedena teorie, jež se vztahuje ke konvolučním rekonstrukčním metodám. Zásadní přínos článku je exaktní matematický přístup k Radonově inverzní transformaci, jenž je založen na pojmu regularizace funkce a zobecněné funkce. Tento přístup pak přirozeně vede i k použití zobecněné Fourierovy transformace.

Uplatnění teorie je ukázáno na řadě počítačových simulací.

Authors' addresses: Jiří Jelínek, M. Sc., Ph. D., Department of Applied Sciences in Medicine, University of Alberta, Edmonton, Alberta T6G 2G3, Canada (on leave from Institut klinické a experimentální medicíny, Vídeňská 800, 146 22 Praha 4, ČSSR); RNDr. *Karel Segeth,* CSc., Matematický ústav ČSAV, Žitná 25, 115 67 Praha 1, ČSSR; Prof. *T. R. Overton,* Department of Applied Sciences in Medicine, University of Alberta, Edmonton, Alberta T6G 2G3, Canada.